ResearchGate

See discussions, stats, and author profiles for this publication at: https://www.researchgate.net/publication/359860447

Experimental and Numerical Investigation of Bridge Configuration Effect on Hydraulic Regime

Article *in* International Journal of Civil Engineering · April 2022

DOI: 10.1007/s40999-022-00715-2

CITATIONS
17

READS
169

4 authors, including:

Mehmet Ardiclioglu
26 PUBLICATIONS **218** CITATIONS

SEE PROFILE

Erion Periku
Epoka University
20 PUBLICATIONS **57** CITATIONS

SEE PROFILE

Alban Kuriqi
University of Lisbon
156 PUBLICATIONS **3,392** CITATIONS

SEE PROFILE

Some of the authors of this publication are also working on these related projects:

Project Special Issue "Renewable Energy Proliferation and Ecosystem Conservation Nexus" View project

Project Special Issue "Climate Extremes: Human-Environment Consequences and Adaptation Measures" View project

All content following this page was uploaded by Alban Kuriqi on 22 November 2022.

The user has requested enhancement of the downloaded file.

International Journal of Civil Engineering
https://doi.org/10.1007/s40999-022-00715-2

RESEARCH PAPER

Experimental and Numerical Investigation of Bridge Configuration Effect on Hydraulic Regime

Mehmet Ardiclioglu[1] · Arzu M. W. Mohamed Hadi[2] · Erion Periku[3] · Alban Kuriqi[4]

Received: 29 November 2021 / Revised: 18 February 2022 / Accepted: 22 March 2022
© Iran University of Science and Technology 2022

Abstract

The presence of a bridge structure in the river induces changes in the natural geometry of the river cross section by, therefore, altering the hydraulic regime significantly and causing the so-called backwater effect. Nevertheless, the effect of the bridge configuration on the hydraulic regime is barely studied. Therefore, the main objective of this study is to investigate the variations in the water surface profile and flow velocity due to the bridge structure configuration. For this purpose, the water surface profile and flow velocity on the upstream and downstream of the bridge were investigated for five flow discharges and four different bridge spans ($M = b/B = 0.58, 0.67, 0.75, 0.83$). In addition, the relationships between the bridge's upstream and downstream average velocities were investigated. The analysis was carried out experimentally and numerically using the HEC-RAS model. The overall average velocity difference upstream of the bridge section was − 92.59%, while downstream of the bridge was determined as − 11.95%. So, the average velocities determined by HEC-RAS were considerably overestimated at the upstream part of the bridge. Linear relationships were identified for the average downstream and upstream measured velocities in the different openings. The correlation coefficients (R^2) were significantly high for considered for all tested b/B ratios. Manning roughness coefficient $n = 0.01$ was found suitable for smooth open channel; nevertheless, a higher n value should be considered non-smooth open channel. The solution-oriented findings from this study might be helpful for engineers by assisting them to reduce uncertainties in the dimensioning of bridges structures.

Keywords Bridge failure · Bridge scouring · Flood vulnerability · HEC-RAS · River hydraulics

Abbreviations

A	Submerged cross-section's area (m^2)
α	Velocity weighting coefficient (–)
C	Expansion or contraction loss coefficient (–)
1D/2D	One dimensional/two dimensional
F_r	Froude number (–)
g	Gravitational acceleration (m/s^2)
h	Water depth (m)
h_e	Energy head loss (m)
h_n	Uniform water depth (cm)
HEC-RAS	River Analysis System (RAS), developed by Hydrologic Engineering Center (HEC) of U.S. Army Corps of Engineers
L	Distance between cross section (m)
n	Manning's roughness coefficient ($s/m^{1/3}$)
Q	Flow discharge (m^3/s)
R	Hydraulic radius (m)
R_e	Reynolds number (–)
ε	Average difference (%)
S	Channel's slope (m/m)
S_f	Friction slope (m/m)
V	Mean flow velocity (m/s)
$V_{downst.}$	Flow velocity downstream (m/s)

✉ Alban Kuriqi
alban.kuriqi@tecnico.ulisboa.pt

Mehmet Ardiclioglu
mardicli@yahoo.com

Arzu M. W. Mohamed Hadi
hadihydro@gmail.com

Erion Periku
erionperiku@gmail.com

1 Independent Research, Kayseri, Turkey

2 Environmental and Pollution Department, Kirkuk Technical College, NTU, Kirkuk, Iraq

3 Independent Research, Tirana, Albania

4 CERIS, Instituto Superior Técnico, University of Lisbon, 1649-004 Lisbon, Portugal

Published online: 10 April 2022

V_{HEC}	Flow velocity estimated with HEC-RAS (m/s)
$V_{meas.}$	Flow velocity measured in the flume (m/s)
$V_{upst.}$	Flow velocity upstream (m/s)
W_b	Bridge deck width (cm)
WSPRO	Water surface profile (m)
Z	River elevation inverts (m)

1 Introduction

Bridges represent a large financial investment and provide an essential service to the community and economy. However, at the same time, bridges are vulnerable structures of transportation networks exposed to multiple hazards, and their failure can severely impact the functionality of the transport system [1, 2]. Being such essential structures, they require accurate design, regular investigation, monitoring, and assessment to ensure good condition and functionality [3, 4].

The stability and serviceability integrate the bridge's superstructure and substructure [5]. Despite their importance, many bridges are aging quickly due to multiple reasons, e.g., increasing traffic, dynamic impulses on the bridge substructure elements, extreme scouring around the abutments or piers, heavy rainfall, floods, or extreme temperatures, which are expected to intensify due to climate change and human-induced factors [3, 4, 6–8].

Often, incorrect design is a prevalent factor of early bridge aging and failure [9, 10]. However, in most cases, although the bridge may be correctly designed and built, it can be damaged or collapsed due to other factors such as flooding and debris that can damage different components of a bridge that lead to the failure of the entire structure. Taking into account that more than one bridge may fail along a river in the same region, during an extreme event, closure of river-crossings can lead to severe network disruption due to very limited or no other diversion alternatives. In this context, flood-induced scouring has been identified as the predominant cause of bridge failure in many countries [1, 3, 8].

Even though abutment and some of the bridge piers are usually placed on floodplains and remain unsubmerged during dry seasons nevertheless, during the wet season, floods may cause a substantial rise in water level and lead to considerable macro-turbulence around the substructure elements of the bridge [11]. Those flow characteristics are leading factors for sediment scouring on alluvial beds by altering the channel morphology and inducing serious scouring [8, 12]. In the United States, more than 60% of bridge failure happens due to scouring [13, 14]. The number of reported bridges failure due to water damage is six times that of overload and 20 times that of earthquakes [1, 15]. Also, in Europe, floods are the main cause of bridges failure [16]. Similarly, bridge failure causes are observed in other regions, such as South America [17] and Asia [18–20]. To minimize the risk of failure, the hydraulic requirements of a stream crossing during the development, construction, and maintenance phases of bridges must be carefully addressed.

Thus, hydraulic regime through bridges is an essential factor for computing water surface profiles and, consequently, the correct bridge design. Accurate computation of the water surface profiles at a bridge structure is essential for well-functioning the bridge itself, safety utilization during high-flow discharges, flood-induced damage reduction, stream stability, and controlling the scouring evolution, among others [21–23].

For better flood prediction and adopting the proper mitigation and protection measures, it is critical to have comprehensive information about a given stream's hydrological and hydraulic characteristics. Bridges are of various types and constructed on natural rivers characterized by different regimes; therefore, planning, design, and construction should be handled carefully according to the river's flow regime type [24, 25]. The optimal bridge design needs accurate estimation of water level fluctuations and hydraulic regime analysis using experimental and modeling tools [26–29].

The opening formed by the bridge's elements must be capable of conveying the high-flow discharges. For this purpose, considering the structure's safety but at the same time, the cost, crucial elements of the bridge such as the foundation depths piers, geometric of the elements, and the highest point on the low chord of the bridge opening must be determined carefully. Hydraulic head acting on bridge's elements are relatively small compared to the structural load. However, hydraulic influence around the bridge due to its geometrical characteristics and infrastructure elements negatively affects the structure itself [30]. A bridge designed with a high safety factor may cause more afflux on the upstream, increasing the cost of river regulation structures [31].

Therefore, it is crucial to develop more cost-effective recommendations to reduce the construction cost and ensure the well-functioning of the bridge structures. While some bridge openings may induce relatively uniform flow velocity across the entire bridge opening, in most instances, there are wide variations in the velocity profile. In some flow segments, e.g., near the center of the stream, the velocity may be considerably higher than the average

velocity [22, 30]. Thus, the changes in the flow due to the geometric bridge structure should be carefully examined.

A handful of experimental and numerical studies investigate the influence of the flow regime around piers groups and other substructure elements [7, 21–23, 30, 32]. Ardiclioglu, Seçkin and Seçilir [33] investigated the effects of bridge structures on maximum afflux conducting several experimental tests at a laboratory channel. Polynomial equations for maximum afflux were obtained based on flow depth, Froude number, and slope. Hadi and Ardiclioglu [32] investigated the maximum afflux through experimental tests and modeling in the HEC-RAS package. Namely, they conducted laboratory experiments considering ten flow discharges in a smoothed channel. The hydraulic parameters computed with HEC-RAS demonstrate to be closer to the measured values for maximum afflux and water surface profiles for large openings. Also, Hadi and Ardiclioglu [32] found that when the opening ratio increases, the position where maximum affluxes were observed initially also shifted upstream of the channel.

Although hydraulic models enable us to conduct high-performance computations at a different scale, still the input data plays a crucial role in the accuracy of results [24, 34]. In this regard, determining correct roughness represented by Manning's *n* coefficient is crucial but, at the same time, a challenging task [34, 35]. Especially in hydraulic modeling of bridge structures, the determination of Manning's *n* coefficient is challenging and very sensitive as it affects the bridge's dimensions. Thus, roughness influences the water surface profile, which dictates the dimensions of specific structural elements of the bridge [22, 23].

Roughness can be affected by factors such as the geomorphology of the river and the opening of the bridge's spans, among others [13, 34, 36]. While the influence of the geomorphology of the river on roughness is well investigated and reported in the literature, to the best of the authors' knowledge, the influence of the bridge's span opening on the roughness and, consequently, on the hydraulic regime of the flow discharge passing through the bridge is scarcely investigated. Therefore, this study's main objective is to investigate how a bridge's spans opening affect the roughness and other hydraulic parameters, such as water surface profile and velocity, which have a crucial role in designing cost-effective bridges.

Namely, the main objective of this study is to understand the influence of bridge structures equipped with rectangular cross-section elements (i.e., four different bridge spans) on water surface profile and average velocity experimentally and numerically using the HEC-RAS model. Specifically, the water surface profiles and average velocities on the upstream and downstream faces of the bridge for five different discharges and four different bridge spans were investigated. In addition, the relationships between the measured and computed average velocities upstream and downstream of the bridge were investigated. Thus, this study intends to offer a better understanding of hydraulic regime—bridge's substructures elements interactions to assist engineers in designing cost-effective bridges.

2 Materials and Methods

2.1 Experimental Setup

The experiments were performed in a glass-walled rectangular laboratory flume 9.5 m long, 0.6 m wide, and 0.6 m depth at the Laboratory of Hydraulics of Erciyes University, Kayseri, Turkey. The water flow rate by the flume was measured with the support of a UFM-600 type ultra-sound current meter mounted on the pipe, transferring the water from a constant-head tank to the flume entrance [37]. Water surface profiles and velocities were measured using a point gage mounted on a tripod, which can move freely in three dimensions (Fig. 1a).

Flow velocities were measured using the Streamflow Velocity Meter 400 type "Low-Speed Propeller Probe" [38], placed on the tripod (Fig. 1b). To precisely determine the point velocity in the measurements, the average frequency was determined every 10 s on the digital display, as seen in Fig. 1c, this process was repeated three times for each point, and the point velocities were then determined with the help of the average of these three frequencies.

Bridge models with rectangular cross section and four openings, i.e., spans ($M = b/B = 0.58$, 0.67, 0.75, 0.83) were used in the experiments, where b; is the bridge span and B; is the channel width (60 cm). The bridge deck width, made of wooden material, is $W_b = 5$ cm. The dimensions and the configuration of the bridge's rectangular spans are given in Fig. 1a. The bridge model was placed at the 6th meter of the channel to determine average upstream and downstream velocities and see the effect of the bridge structure in the water surface profile fluctuations. Velocity measurements were made at the 1 cm in front of the upstream and downstream faces of the bridge section at the middle of the bridge span. Point velocities were measured for five different steady flow conditions, as given in Table 1.

Where Q = discharge, h_n = uniform water depth, V (Q/A) = mean flow velocity, S = channel's slope, $R_e(4VR/\upsilon)$ = Reynolds number, and $\mathrm{Fr}(V/\sqrt{gh_n})$ = Froude number. The average velocities were measured for five discharges and four different b/B ratios on the upstream and downstream parts in the middle of the spans. Mean velocity V, in

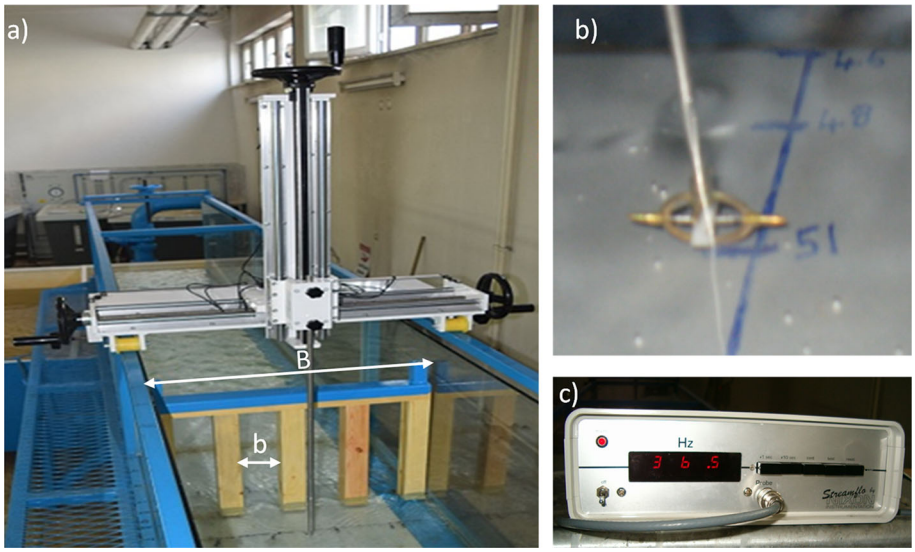

Fig. 1 The experimental flume and measurement equipment

Table 1 Flow properties measured for different flow conditions

Test	Q (lt/s)	h_n (cm)	$V = Q/A$ (m/s)	S	Re	Fr
1	7.16	3.45	0.346	0.001	42,387	0.595
2	14.2	5.31	0.446	0.001	79,634	0.618
3	21.23	6.88	0.514	0.001	113,990	0.626
4	28.47	8.34	0.569	0.001	147,043	0.629
5	34.27	9.42	0.606	0.001	172,150	0.631

a vertical, is obtained from velocity measurements at several points at a given vertical. In the vertical–velocity curve method, a series of velocity observations at given points well distributed between the water surface and the stream bed was conducted at each chosen vertical [34]. The mean velocity in the vertical is obtained by measuring the area between the curve and the ordinate axis and dividing the area by the flow depth in this vertical using Eq. (1).

$$V = \frac{\sum \frac{(v_i + v_{i+1})}{2} h_i}{h}. \tag{1}$$

In this Equation, two consecutive velocities, v_i and v_{i+1}, and for a depth h_i, show the distance between consecutive velocities measurements points.

2.2 Numerical Simulations

The HEC-RAS model was used to conduct the hydraulic simulation of the flow regime passing under the bridge. In this study, since the analysis consists in modeling a relatively small laboratory-scale channel and bridge, the cross-sections are taken at a relatively small span along the channel to characterize the carrying capacity. The geometry of the channel, normal depth with bed slope, and flow resistance are required for simulating uniform flow using a hydraulic model. Using the bridge geometrical data menu, bridge location on the channel was selected along with all the details of the experimental model. The bridge itself explained above is composed of four-span with different dimensions. Water surface profiles in HEC-RAS are computed from one cross section to the next by solving the energy equation to a body of water enclosed by two cross sections at locations 1 and 2 as follows, Eq. (2):

$$h_2 + Z_2 + \frac{\alpha_2 V_2^3}{2g} = h_1 + Z_1 + \frac{\alpha_1 V_1^3}{2g} + h_e \tag{2}$$

where h is the water depth at cross sections, Z is the river's elevation inverts, V is the mean flow velocity, α is the velocity weighting coefficient, g is the gravitational acceleration, and h_e is the energy head loss. The energy head loss between two cross sections is encompassed of friction losses and contraction and expansion losses expressed as follows, Eq. (3):

$$h_e = LS_f + C\left(\frac{\alpha_2 V_2^2}{2g} - \frac{\alpha_1 V_1^2}{2g}\right), \tag{3}$$

where L is the distance between cross Sects. 1 and 2 along the direction of the flow, S_f is the friction slope between two cross sections, which is computed using Manning's equation as follows, Eq. (4):

$$Q = \frac{1}{n} A R^{2/3} S_f{}^{1/2}, \tag{4}$$

where Q is the flow discharge, n is the Manning roughness coefficient; A is the flow area, R is the hydraulic radius, and

C is the expansion or contraction loss coefficient. The Manning roughness coefficient n was calibrated for bridge modeling with the HEC-RAS model in the smooth open channel. Manning's n coefficient was set within the allowable range (0.0085–0.0120) for the smooth channel used in the laboratory work [24, 35]. In the bridgeless open-channel model, different Manning n values were iteratively tested [35]. The average velocities were determined in the 6.5 m of the channel where the bridge was placed, in the middle section of the channel (y = 30 cm). Relative differences between measured and computed average velocities for four bridge spans are calculated using Eq. (5):

$$\varepsilon(\%) = \frac{V_{\text{meas.}} - V_{\text{HEC}}}{V_{\text{meas.}}} \times 100. \tag{5}$$

The HEC-RAS model assumes that a contraction occurs whenever the flow velocity downstream is greater than the upstream. When the change in the river cross-section is small and the flow is subcritical, the contraction and expansion coefficients are equal to 0.1 and 0.3, respectively [24]. In a more abrupt change, such as these occurring at bridges, the used values are 0.3 and 0.5, respectively [22, 36, 39]. However, the HEC-RAS model will automatically select the appropriate equation, depending on how the bridge structure operates hydraulically. The first scenario could be when only the upstream side of the bridge is in contact with the water; the second is when the bridge contraction is flowing full [23]. Manning roughness coefficient was determined iteratively for each case. Flow discharges were tested in the flume until the differences between simulated and observed water surface profile and velocity, respectively, were relatively small [22, 35, 39]. Thus, for each bridge configuration (i.e., number and the spans' ratio), an appropriate Manning's n coefficient was recommended to represent the roughness induced due to the number of piers introduced in the bridge structure.

3 Results and Discussion

3.1 Characterization of the Measured and Simulated Water Surface Profiles

Figure 2 shows the energy (i.e., only simulated) and water surface profiles measured during the experimental work and computed with the HEC-RAS model for different configurations (i.e., numbers and spans' ratio) of the bridge structure and flow discharges. In general, results show no considerable fluctuation of water surface profile upstream of the bridges at four configurations and for five flow discharges scenarios. In contrast, downstream of the bridge, the water surface profile fluctuations increase with the increase of the spans' ratio and flow discharge passing through the bridge structure. The highest fluctuations of the water surface profile occur near the bridge contraction, then it stabilizes.

Figure 3 shows the variability of the water surface profile differences between measured and computed with HEC-RAS along the flume for four bridge configurations and five flow discharges, respectively.

Results show that despite the iterative computations conducted with HEC-RAS to assign the most accurate Manning's n value, the difference between measured and simulated water surface profile increases with increasing the spans' ratio in the bridge structure. Thus, making the estimation of the water surface profile more challenging with hydraulic models such as HEC-RAS. Nevertheless, in the bridges with a relatively small span ratio, except for Q = 7.16 l/s, the water surface profile difference variability is smaller than other bridge configurations (i.e., with a higher span ratio). In real cases, although not very common, the high uncertainty of water surface profile estimation with hydraulic models during low flow could be due to random obstacles such as debris, large stones, and woods near the bridge piers, which are overlooked [23, 39]. However, water surface profile differences for low flows are generally smaller than higher flows. The slight difference in water surface profile in low flows is due to low turbulence and eddies, especially near the bridge piers [21, 24, 39].

In contrast, higher turbulence and eddies occur close to the bridge piers during high-flow discharges that significantly alter the water surface profile both upstream and downstream of the bridge, particularly close to the piers. In prolonged flood events, it may cause severe damages or, in the worst case, failure of the bridge structure itself [13, 29, 30]. Thus, during high-flow events, in bridges with more than one span and a high ratio of the span, the uncertainty of water surface profile estimation with hydraulic models such as HEC-RAS is higher as the afflux formed upstream of the bridge obstructs the flow and causes higher turbulences and eddies around the bridge's piers and also hydraulic regime in the downstream direction tends to be supercritical [22, 23]. Such undesirable hydraulic effects can be avoided or mitigated by applying collars elements at a different level of the bottom part of the bridge's piers [8, 28]. In the case of bridges with several spans, an overestimation of Manning's n value may slightly increase the cost of the bridge construction; nevertheless, the bridge's safety is significantly higher [30, 39]. Therefore, depending on the number of spans and spans' ratio, also considering the influence of the vegetation and geomorphology, a Manning's n value between 0.01 and 0.07 can be recommended to be used in hydraulic

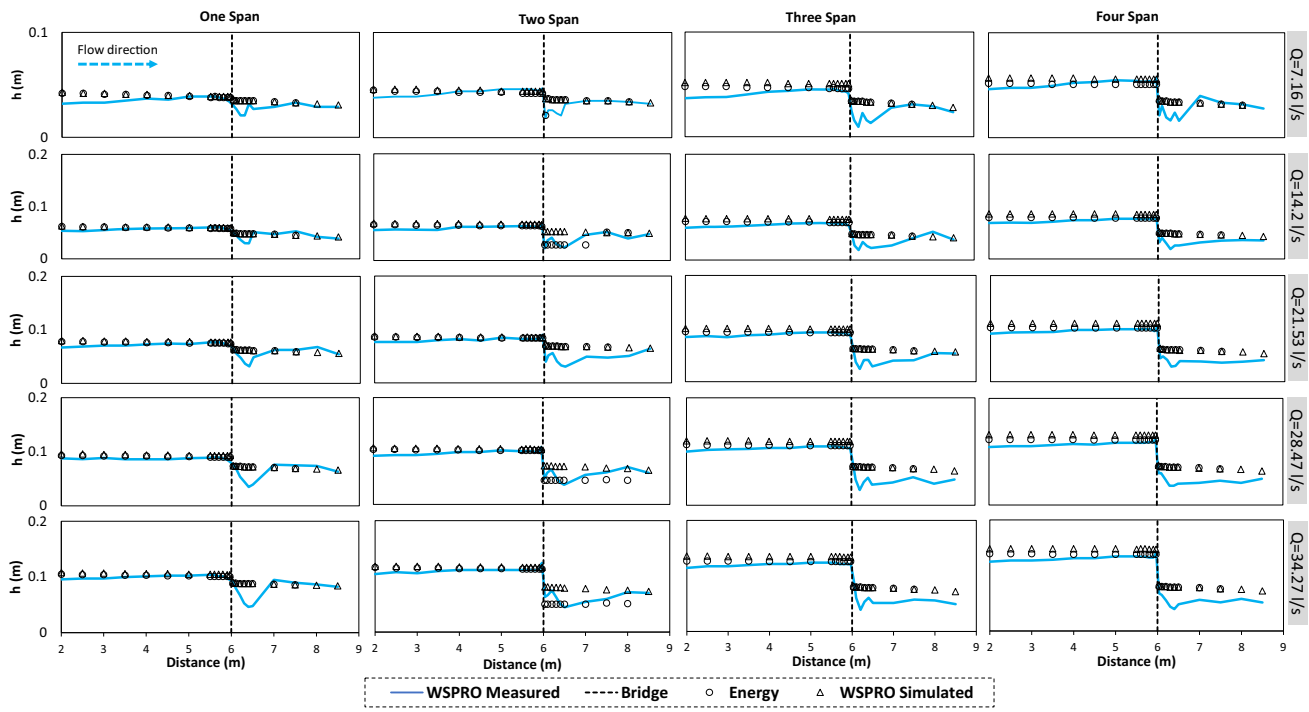

Fig. 2 Energy (simulated) and water surface profiles (WSPRO) measured in the flume and simulated with HEC-RAS for different bridge configurations and flow discharge scenarios

models for estimating the water surface profile near the abridge structure [21, 22, 35].

3.2 Comparison of the Measured and Simulated Average Velocities

As shown in Fig. 4a, average velocities for the two-span bridge were found as 55.3 cm/s at y = 16.3 cm. The same method calculated average vertical velocity as 95.5 cm/s at y = 16.3 cm downstream of the bridge (Fig. 4b).

As shown in Fig. 5, when there is no bridge in the experimental channel, measured and simulated average velocities by HEC-RAS are relatively close for a Manning's n = 0.01.

The average difference between measured and computed velocities was found as − 0.71. Thus, in the case of laboratory conditions for smooth open-channel flows, it would be appropriate to consider Manning n = 0.01. Nevertheless, the same recommendation is not valid for non-smooth open-channel flows as many geomorphological factors influence roughness [23, 35]. As mentioned in Sect. 2.2, we tested five flow discharges and four bridge openings to conduct HEC-RAS simulations. Once the necessary data were inserted, the program became ready to run a steady flow simulation. After the computations were completed, the average velocities were determined at the middle of the openings (Fig. 6). As shown in Fig. 6, average velocities at the middle of the opening at y = 16 cm for upstream and downstream were calculated as $V_{\text{upst.}}$ = 1.12 and $V_{\text{downst.}}$ = 1.15 m/s, respectively, for the fifth flow discharge scenario as that was the case where higher water surface profile fluctuations occurred.

In this study, since the experimental channel is relatively small, the velocity variations in the cross section near the bridge's opening are small but abrupt; namely, it varies from 0.4 to 1.2 m/s. The simulated average velocities in each bridge span with HEC-RAS were compared with the measurements for five flow discharge scenarios (Table 2).

As shown in Table 2, the differences between measured and simulated velocities at the bridge upstream are high and significantly affected by the spans' ratio. The average value of these differences is − 92.59%. In contrast, the differences between measured and computed velocities downstream of the bridge were relatively small. The average value of downstream velocity difference was determined as − 11.95%. Negative values mean that the measurement values are smaller than those calculated by HEC-RAS. Figure 7 shows the graphical distributions of velocity differences in the span mid-sections on the upstream and downstream faces for a two-span bridge (b/B = 0.75).

Figure 7a shows the distribution of differences determined at y = 16.3 and 43.8 cm on the upstream part of the bridge. As shown in Fig. 7a, the velocity differences of both openings are close to each other and high (− 111.59%) for b/B = 0.75. The velocity differences

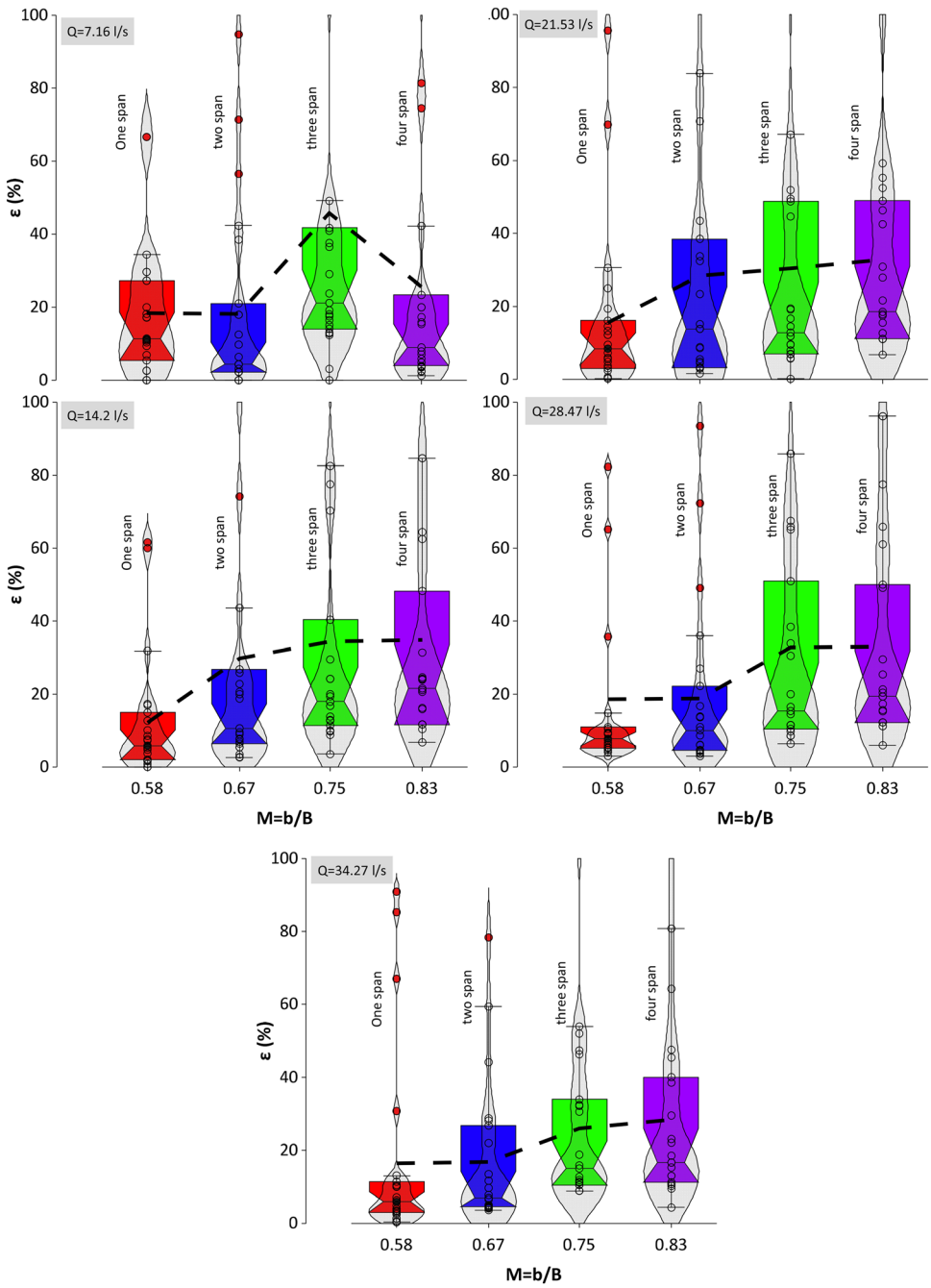

Fig. 3 Water surface profile variability measured and computed with HEC-RAS along the flume for four bridge configurations and five flow discharges scenarios

determined in both openings at the downstream section of the bridge are again close to each other and smaller than the upstream face (− 31.34%). As presented in Table 2, a similar trend was observed for other openings.

3.3 Relation of the Upstream and Downstream Average Velocities

Relation of the velocities measured at the downstream and upstream spans of the bridge was investigated. As discussed above, the highest variability of the water surface profile was observed both experimentally and numerically for the bridge's span *b/B* = 0.75. Therefore, we wanted to see if and how this high variability in water surface profile

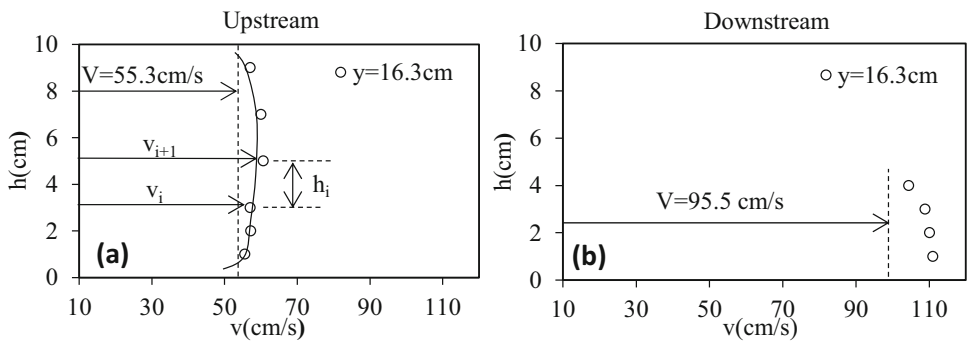

Fig. 4 Upstream and downstream point velocities at fifth measurement for two spans bridges

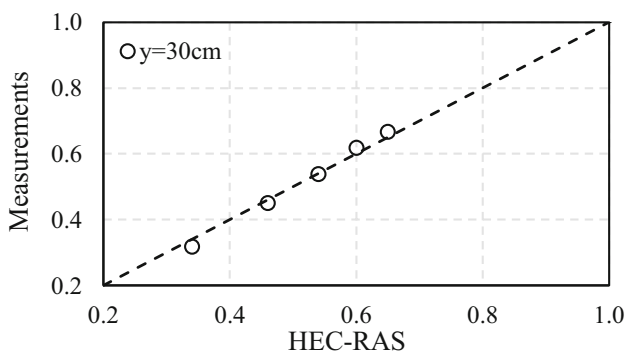

Fig. 5 Measured and simulated average velocities for five flows scenarios

affects flow velocity upstream and downstream of the bridge. As shown in Fig. 8, there is a linear relationship between downstream and upstream mean velocities that can be defined through the linear equation shown in the respective figure. This finding indicates that water surface profile variations significantly affect flow velocities at both sides (i.e., upstream and downstream) of the bridge and almost at the same degree [14, 27]. Thus, for b/B = 0.75, the a and b coefficients of the respective equation were determined as 2.035 and -0.144, respectively.

As shown in Table 3, the correlation coefficient for this relationship is relatively high (R^2 = 0.918).

Similarly, values of determination coefficient (R^2) were found for other opening ratios (Table 3). As can be seen from the table, coefficient a gets more prominent as the opening ratio (b/B) gets smaller. R^2 values were determined to be relatively high for all analyzed b/B ratios.

We acknowledge that despite the significant contribution of this study, we identify some limitations that can be addressed in future studies. Since the experimental work was conducted in a smooth laboratory flume. There are various uncertainties in the flume interactions' bridge-flow discharge and morphology. Namely, our analysis was focused solely on the interaction of flow discharge with the bridge structure itself, assuming no friction with the surrounding environment. However, in the natural environment, as mentioned above, the geomorphology, including the bathymetry, type of vegetation, and geological formation of the river, has a considerable influence on the hydraulic regime of the flow closer to the bridge structure; in other words, it influences the roughness [23, 35]. To the authors' knowledge, previous works assume the flow velocity, or scour depth, as the intensity measure that does not account for the streaming characteristic effectively. Thus, an arbitrary velocity increase does not represent the field flow velocity. Usually, in field conditions, flow velocity plateaus may even drop after the river's overflow [30]. One of the critical disadvantages of flow velocity is that it does not represent the hydraulic parameters in the river uniquely; for example, the same flow velocity may occur for different hydraulic conditions. Moreover, the flow velocity is not easy to measure in the natural field or readily available for rivers. Nevertheless, considering this study's specific objective, we believe that the limitations above do not jeopardize the significance of this study.

4 Conclusion

Experimental and HEC-RAS bridge modeling was carried out to investigate the effects of bridge structures configuration on the water surface profile and the average flow velocities. For this purpose, the water surface profile and the average flow velocities upstream and downstream of the bridge at five flow discharges and four bridge spans ($M = b/B$ = 0.58, 0.67, 0.75, 0.83) were considered. The following main conclusions can be summarized from this study.

- Water surface profile variability and differences were higher for higher spans ratios and flow discharges. The opposite occurred for low flows.
- Manning roughness coefficient n = 0.01 was found suitable for smooth open-channel flows; nevertheless,

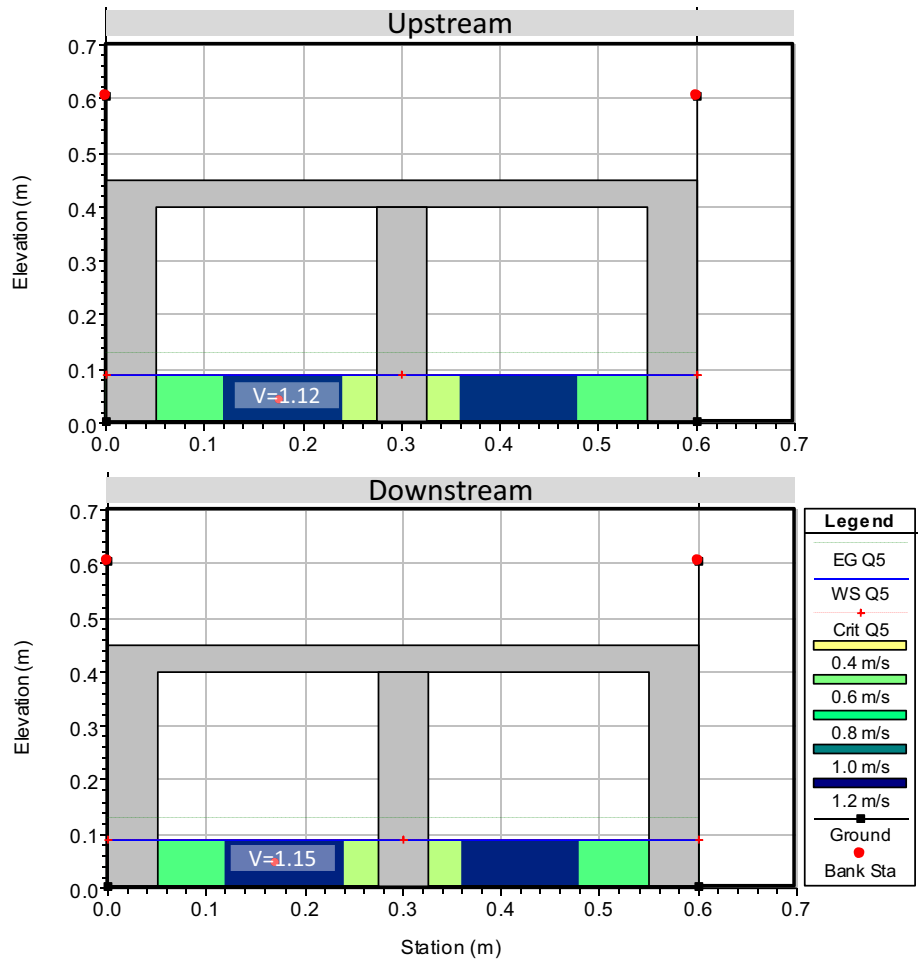

Fig. 6 Average velocities for two opening bridges at y = 16 cm for upstream and downstream cross sections and flow discharge Q = 34.27 l/s

Table 2 Differences between measured and simulated average velocities

b/*B*	Error (%)	
	Upstream	Downstream
0.58	− 127.06	− 7.78
0.67	− 98.01	− 8.70
0.75	− 111.59	− 31.34
0.83	− 33.70	0.03
Average	− 92.59	− 11.95

depending on the geomorphological conditions, a higher n value should be considered when conducting hydraulic simulations for a non-smooth open-channel flow or a natural stream.

- Average velocities in bridge spans can be easily determined with HEC-RAS for smooth open-channel flows; nevertheless, this process might be challenging for non-smooth open-channel flows as the roughens varies in space and time.
- The average differences between the measured and simulated velocities for five flow discharges were high for both sides of the bridges.
- The overall average velocity difference at the upstream bridge section is − 92.59%. In other words, the average velocities determined by HEC-RAS were overestimated.
- The overall average velocity differences in the downstream section of the bridge were determined as − 11.95%, relatively small compared to the upstream part.
- A linear relationship between downstream and upstream measured mean velocities was observed for each span.
- The slopes of the linear relationship (i.e., a coefficient) become higher as the bridge span ratio gets smaller. The correlation coefficients of these relations R^2 were pretty high for all bridge's span ratios.

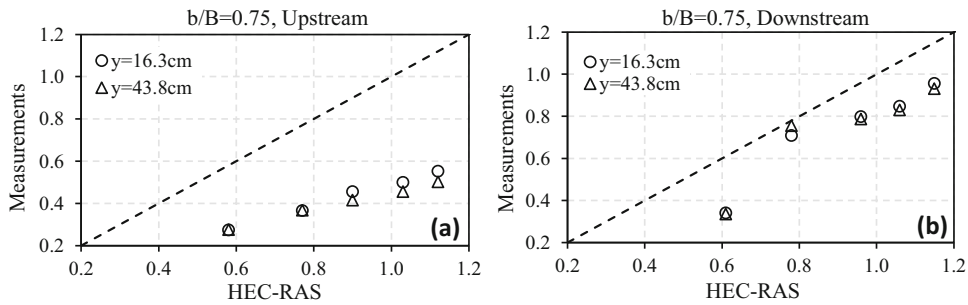

Fig. 7 Relative differences for measured and computed mean velocities in the span mid-sections

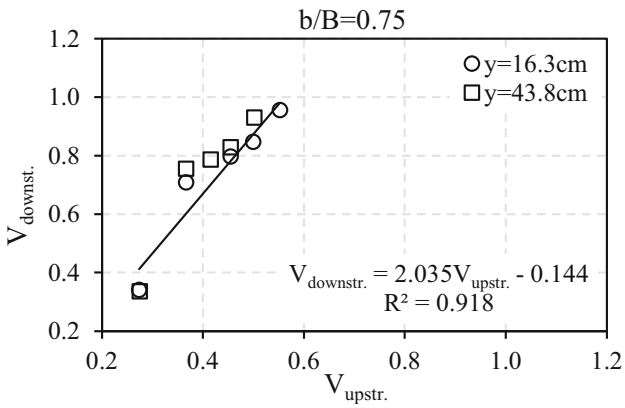

Fig. 8 Relation between measured and computed mean velocities for *b/B* = 0.75

Table 3 Relation between downstream and upstream measured average velocities

b/B	*a*	*b*	R^2
0.83	1.358	− 0.004	0.987
0.75	2.035	− 0.144	0.918
0.67	2.579	− 0.215	0.972
0.58	3.149	− 0.255	0.893

Overall, this study concludes that hydraulic models overestimate several hydraulic parameters, especially when used to model the hydraulic regime of flow discharge passing through hydraulic structures such as bridges. Nevertheless, the accuracy of the results greatly depends on the flow regime type and accurate representation of the channel roughens. As the findings of this study revealed, the differences were quite remarkable from upstream to downstream of the structure and significantly affected by the opening ratio. However, considering the importance of bridge structures, those overestimations are irrelevant. Accurate determination of the roughness represented by Manning's *n* coefficient is crucial in the correct design of bridges and other hydraulic structures. Therefore, future studies would consider the influence of the geomorphology and vegetation on the roughness. Finally, this study's methodology and solution-oriented findings might help engineers accurately design bridge structures constructed in natural or artificial channels.

Acknowledgements Alban Kuriqi acknowledges the Portuguese Foundation for Science and Technology (FCT) support through PTDC/CTA-OHR/30561/2017 (WinTherface).

Author contributions MA, AMWMH, EP, and AK: conceptualization, methodology, investigation, formal analysis, data curation, visualization, writing—original draft. MAAK: writing—review and editing, resources, supervision.

Funding This study did not receive any funding.

Availability of Data and Materials The first author should be contacted for the data.

Code Availability The first author should be contacted for the data.

References

1. Argyroudis SA, Mitoulis SA (2021) Vulnerability of bridges to individual and multiple hazards-floods and earthquakes. Reliab Eng Syst Saf 210:107564. https://doi.org/10.1016/j.ress.2021.107564
2. Breccolotti M, Natalicchi M (2021) Bridge damage detection through combined quasi-static influence lines and weigh-in-motion devices. Int J Civ Eng 19(11):1–14. https://doi.org/10.1007/s40999-021-00682-0
3. Wu C, Wu P, Wang J, Jiang R, Chen M, Wang X (2020) Critical review of data-driven decision-making in bridge operation and maintenance. Struct Infrastruct Eng 18(1):47–70. https://doi.org/10.1080/15732479.2020.1833946
4. Sun L, Shang Z, Xia Y, Bhowmick S, Nagarajaiah S (2020) Review of bridge structural health monitoring aided by big data and artificial intelligence: from condition assessment to damage detection. J Struct Eng 146(5):04020073. https://doi.org/10.1061/(ASCE)ST.1943-541X.0002535
5. Shaker F, Rahai A (2019) Substructure responses of a concrete bridge with different deck-to-Pier connections. Int J Civ Eng 17(11):1683–1695. https://doi.org/10.1007/s40999-019-00455-w
6. Ardiclioglu M, Genc O (2015) Investigation of bridge afflux on urban transport by experiments and HEC-RAS package. In: (Ed.)^(Eds.), 7th Urban infrastructure symposium. Trabzon, Turkey, pp 1–12

7. Ghaderi A, Daneshfaraz R, Dasineh M (2019) Evaluation and prediction of the scour depth of bridge foundations with HEC-RAS numerical model and empirical equations (Case Study: Bridge of Simineh Rood Miandoab, Iran). Eng J 23(6):279–295. https://doi.org/10.4186/ej.2019.23.6.279
8. Pizarro A, Manfreda S, Tubaldi E (2020) The science behind scour at bridge foundations: a review. Water 12(2):374. https://doi.org/10.3390/w12020374
9. Hai DT, Yamada H, Katsuchi H (2007) Present condition of highway bridges in Vietnam: an analysis of current failure modes and their main causes. Struct Infrastruct Eng 3(1):61–73. https://doi.org/10.1080/15732470500254774
10. Wardhana K, Hadipriono FC (2003) Analysis of recent bridge failures in the United States. J Perform Constr Facil 17(3):144–150. https://doi.org/10.1061/(ASCE)0887-3828(2003)17:3(144)
11. Yang Y, Xiong X, Melville BW, Sturm TW (2021) Dynamic morphology in a bridge-contracted compound channel during extreme floods: effects of abutments, bed-forms and scour countermeasures. J Hydrol 594:125930. https://doi.org/10.1016/j.jhydrol.2020.125930
12. Cao F, Tao Q, Dong S, Li X (2020) Influence of rain pattern on flood control in mountain creek areas: a case study of northern Zhejiang. Appl Water Sci 10(10):224. https://doi.org/10.1007/s13201-020-01308-x
13. Deng L, Cai C (2010) Bridge scour: Prediction, modeling, monitoring, and countermeasures. Pract Period Struct Design Constr 15(2):125–134. https://doi.org/10.1061/(ASCE)SC.1943-5576.0000041
14. Alemi M, Maia R (2018) Numerical simulation of the flow and local scour process around single and complex bridge Piers. Int J Civ Eng 16(5):475–487. https://doi.org/10.1007/s40999-016-0137-8
15. Khandel O, Soliman M (2019) Integrated framework for quantifying the effect of climate change on the risk of bridge failure due to floods and flood-induced scour. J Bridg Eng 24(9):04019090. https://doi.org/10.1061/(ASCE)BE.1943-5592.0001473
16. Mitoulis SA, Argyroudis SA, Loli M, Imam B (2021) Restoration models for quantifying flood resilience of bridges. Eng Struct 238:112180. https://doi.org/10.1016/j.engstruct.2021.112180
17. Diaz EEM, Moreno FN, Mohammadi J (2009) Investigation of common causes of bridge collapse in Colombia. Pract Period Struct Design Constr 14(4):194–200. https://doi.org/10.1061/(ASCE)SC.1943-5576.0000006
18. Wu T-R, Wang H, Ko Y-Y, Chiou J-S, Hsieh S-C, Chen C-H, Lin C, Wang C-Y, Chuang M-H (2014) Forensic diagnosis on flood-induced bridge failure. II: framework of quantitative assessment. J Perform Constr Facil 28(1):85–95. https://doi.org/10.1061/(ASCE)CF.1943-5509.0000393
19. Garg RK, Chandra S, Kumar A (2020) Analysis of bridge failures in India from 1977 to 2017. Struct Infrastruct Eng 18(3):1–18. https://doi.org/10.1080/15732479.2020.1832539
20. Schaap HS, Caner A (2021) Bridge collapses in Turkey: causes and remedies. Struct Infrastruct Eng. https://doi.org/10.1080/15732479.2020.1867198
21. Noor M, Arshad H, Khan M, Khan MA, Aslam MS, Ahmad A (2020) Experimental and HEC-RAS modelling of bridge Pier scouring. J Adv Res Fluid Mech Thermal Sci 74(1):119–132. https://doi.org/10.37934/arfmts.74.1.119132OpenAccess
22. Bonner VR (1996) Bridge hydraulic analysis with HEC-RAS. In: (Ed.)^(Eds.). US Army Corps of Engineers, Hydrologic Engineering Center, USA
23. Brunner GW, Hunt JH (1995) A comparison of the one-dimensional bridge hydraulic routines from HEC-RAS, HEC-2 and WSPRO. In: (Ed.)^(Eds.). Hydrologic Engineering Center Davis CA, USA, pp. 1–80
24. Brunner GW (2002) Hec-ras (river analysis system). In: (Ed.)^(Eds.), North American Water and Environment Congress & Destructive Water. ASCE, pp 3782–3787
25. Al-Husseini TR, Hamad HT, Al-Madhhachi A-ST (2021) Effects of an upstream sluice gate and holes in pooled step cascade weirs on energy dissipation. Int J Civ Eng 19(1):103–114. https://doi.org/10.1007/s40999-020-00568-7
26. Tung Y-K, Mays LW (1982) Optimal risk-based hydraulic design of bridges. J Water Resour Plan Manag Div 108(2):191–203. https://doi.org/10.1061/JWRDDC.0000252
27. Benedict ST, Knight TP (2021) Benefits of compiling and analyzing hydraulic-design data for bridges. Transp Res Rec. https://doi.org/10.1177/03611981211023757
28. Ling M, Wang J, Wu M, Cao L, Fu B (2021) Design and modeling of an improved bridge-type compliant mechanism with its application for hydraulic piezo-valves. Sens Actuators A 324:112687. https://doi.org/10.1016/j.sna.2021.112687
29. Abd El-Hady Rady R (2020) Prediction of local scour around bridge piers: artificial-intelligence-based modeling versus conventional regression methods. Appl Water Sci 10(2):57. https://doi.org/10.1007/s13201-020-1140-4
30. Ahamed T, Duan JG, Jo H (2020) Flood-fragility analysis of instream bridges—consideration of flow hydraulics, geotechnical uncertainties, and variable scour depth. Struct Infrastruct Eng. https://doi.org/10.1080/15732479.2020.1815226
31. Sturm TW (2001) Open channel hydraulics. 1. McGraw-Hill, New York
32. Hadi AM, Ardiclioglu M (2018) Investigation of bridge afflux on channels by experiments and HEC-RAS package. Int J Eng Technol 7(4):4829–4832. https://doi.org/10.14419/ijet.v7i4.21068
33. Ardiclioglu M, Seçkin G, Seçilir S (2006) Experimental investigation of the effects of bridge structures on maximum afflux on rivers. In: (Ed.)^(Eds.), 5th GAP Engineering Congress. Şanlıurfa, Turkey, pp. 25–36
34. Ardıçlıoğlu M, Kuriqi A (2019) Calibration of channel roughness in intermittent rivers using HEC-RAS model: case of Sarimsakli creek, Turkey. SN Appl Sci 1(9):1080. https://doi.org/10.1007/s42452-019-1141-9
35. Arcement GJ, Schneider VR (1989) Guide for selecting Manning's roughness coefficients for natural channels and flood plains. US Government Printing Office, Washington DC, pp 1–38
36. Brunner GW, Gibson S (2005) Sediment transport modeling in HEC RAS. Impacts of Global Climate Change. pp 1–12
37. Instrumart, Shop industrial and laboratory instruments, 2022. https://www.instrumart.com
38. HydroMet, Water flow, 2022. https://www.ott.com/products/water-flow-127/
39. Mehta DJ, Yadav SM (2020) Analysis of scour depth in the case of parallel bridges using HEC-RAS. Water Supply 20(8):3419–3432. https://doi.org/10.2166/ws.2020.255

View publication stats